arXiv:hep-ph/0506179v2 29 Jun 2005

Thermalization vs. Isotropization & Azimuthal Fluctuations[1]

Stanislaw Mrówczyński

Institute of Physics, Świętokrzyska Academy ul. Świętokrzyska 15, PL - 25-406 Kielce, Poland and Sołtan Institute for Nuclear Studies ul. Hoża 69, PL - 00-681 Warsaw, Poland

E-mail: mrow@fuw.edu.pl

Abstract.

Hydrodynamic description requires a local thermodynamic equilibrium of the system under study but an approximate hydrodynamic behaviour is already manifested when a momentum distribution of liquid components is not of equilibrium form but merely isotropic. While the process of equilibration is relatively slow, the parton system becomes isotropic rather fast due to the plasma instabilities. Azimuthal fluctuations observed in relativistic heavy-ion collisions are argued to distinguish between a fully equilibrated and only isotropic parton system produced in the collision early stage.

1. Introduction

A matter created in relativistic heavy-ion collisions manifests a strongly collective hydrodynamic behaviour [1], particularly evident in studies of the so-called elliptic flow [2, 3, 4, 5]. Hydrodynamic description requires, strictly speaking, a local thermal equilibrium and experimental data on the particle spectra and the elliptic flow suggest, when analysed within the hydrodynamic model, that an equilibration time of the parton[2] system produced at the collision early stage is as short as 0.6 fm/c [6]. Such a fast equilibration can be explained assuming that the quark-gluon plasma is strongly coupled [7]. However, high-energy density in the collision early stage, when the elliptic flow is generated [8], allows one to believe that the plasma is then weakly coupled due to the asymptotic freedom. Calculations, which assume that the parton-parton collisions are responsible for the equilibration of the weakly interacting plasma, provide an equilibration time of at least 2.6 fm/c [9]. To thermalize the system one needs either a few hard collisions of the momentum transfer of order of the characteristic parton momentum[3], which we denote here as T (as the temperature of equilibrium system), or many collisions of smaller transfer. As discussed in *e.g.* [10], the inverse time scale of the collisional equilibration is of order $g^4 \ln(1/g)\, T$ where g is the QCD coupling constant. However, it has been argued that the equilibration is speeded up by instabilities generated in an anisotropic quark-gluon plasma [11, 12, 13], as growth of the unstable modes is associated with the system's

[1] presented at the workshop *Correlations and Fluctuations in Relativistic Nuclear Collisions*, MIT, April 21-23, 2005

[2] The term 'parton' is used to denote a fermionic (quark) or bosonic (gluon) excitation of the quark-gluon plasma.

[3] Although I consider anisotropic systems, the characteristic momentum in all directions is assumed to be of the same order.

isotropization. The characteristic inverse time of instability development is roughly of order gT for a sufficiently anisotropic momentum distribution [11, 14, 15, 16]. Thus, the instabilities are much 'faster' than the hard collisions in the weak coupling regime. Very recent classical simulation [17] indeed shows effectiveness of the instabilities driven isotropization.

The isotropization should be clearly distinguished from the equilibration process [11]. The instabilities driven isotropization is a mean-field reversible phenomenon which is not accompanied with entropy production. Therefore, the collisions, which are responsible for the dissipation, are needed to reach the equilibrium state of maximal entropy. The instabilities contribute to the equilibration indirectly, reducing relative parton momenta and increasing the collision rate.

It has been recently observed that the hydrodynamic collective behaviour does not actually require local thermodynamic equilibrium but a merely isotropic momentum distribution of liquid components [13]. Thus, there is a question whether a quark-gluon plasma, which is equilibrated nearly immediately after its production as advocated in [7], can be distinguished from the parton system which slowly evolves towards equilibrium being isotropized fast. I argue here that measurements of azimuthal fluctuations, which are generated at the early stage of heavy-ion collisions, can help to distinguish the two scenarios.

In the first part of my talk I review the instabilities driven isotropization. I discuss how the unstable modes are initiated and what is a mechanism responsible for their growth. Dispersion relations of the unstable modes are considered, and it is explained why the development of instabilities is associated with the system's isotropization. In the second part of my talk I discuss the azimuthal fluctuations, arguing that the fluctuations generated in the non-equilibrium isotropic system are much larger than those in the fully equilibrated plasma. Two possible measurements are proposed.

2. Instabilities driven isotropization

Temporal evolution of the electron-ion plasma is plagued by a large variety of instabilities. Those caused by coordinate space inhomogeneities, in particular by the system's boundaries, are usually called the hydrodynamic instabilities while those due to non-equilibrium momentum distribution of plasma particles the kinetic instabilities. Hardly anything is known about hydrodynamic instabilities of the quark-gluon plasma, and I will not speculate about their possible role in the system's dynamics. The kinetic instabilities are initiated either by the charge or current fluctuations. In the first case, the electric field ($\mathbf{E}$) is longitudinal ($\mathbf{E} \parallel \mathbf{k}$, where $\mathbf{k}$ is the wave vector), while in the second case the field is transverse ($\mathbf{E} \perp \mathbf{k}$). For this reason, the kinetic instabilities caused by the charge fluctuations are usually called *longitudinal* while those caused the current fluctuations *transverse*. Since the electric field plays a crucial role in the longitudinal mode generation, the longitudinal instabilities are also called *electric* while the transverse ones *magnetic*.

In the non-relativistic plasma the electric instabilities are usually much more important than the magnetic ones as the magnetic effects are suppressed by the factor v^2/c^2 where v is the particle's velocity. In the relativistic plasma both types of similar strength. The electric instabilities occur when the momentum distribution has more than one maximum while a sufficient condition for the magnetic instabilities is, as discussed below, anisotropy of the momentum distribution. For this reason, the magnetic unstable mode, which is also called Weibel or filamentation instability [18], was argued long ago to be relevant for equilibration of the quark-gluon plasma produced in relativistic heavy-ion collisions [11]. In the remaing part of the section, I am going to explain in detail why the filamentation is relevant and how it speeds up the process of plasma thermalization.

2.1. Seeds of the filamentation

Let me first discuss how the unstable transverse modes are initiated. For this purpose I consider a parton system which is homogeneous but the parton momentum distribution is, in general, not of the equilibrium form, it is *not* isotropic. The system is on average locally colourless but colour fluctuations are possible. Therefore, $\langle j^\mu_a(x)\rangle = 0$ where $j^\mu_a(x)$ is a local colour four-current in the adjoint representation of SU(3) gauge group with $\mu = 0, 1, 2, 3$ and $a = 1, 2, 3, \ldots, 8$ being the Lorentz and colour index, respectively; $x = (t, \mathbf{x})$ denotes a four-position in the coordinate space.

As discussed in detail in [19], the current correlator for a classical system of non-interacting quarks and gluons is

$$M^{\mu\nu}_{ab}(t,\mathbf{x}) \stackrel{\rm def}{=} \langle j^\mu_a(t_1,\mathbf{x}_1) j^\nu_b(t_2,\mathbf{x}_2)\rangle = \frac{1}{8}\, g^2\, \delta^{ab} \int \frac{d^3p}{(2\pi)^3}\, \frac{p^\mu p^\nu}{E_p^2}\, f(\mathbf{p})\, \delta^{(3)}(\mathbf{x}-\mathbf{v}t)\ , \qquad (1)$$

where $(t, \mathbf{x}) \equiv (t_2 - t_1, \mathbf{x}_2 - \mathbf{x}_1)$ and the effective parton distribution function $f(\mathbf{p})$ equals $n(\mathbf{p})+\bar{n}(\mathbf{p})+6n_g(\mathbf{p})$ with $n(\mathbf{p})$, $\bar{n}(\mathbf{p})$ and $n_g(\mathbf{p})$ giving the average colourless distribution function of quarks $Q^{ij}(x,\mathbf{p}) = \delta^{ij} n(\mathbf{p})$, antiquarks $\bar{Q}^{ij}(x,\mathbf{p}) = \delta^{ij}\bar{n}(\mathbf{p})$, and gluons $G^{ab}(x,\mathbf{p}) = \delta^{ab} n_g(\mathbf{p})$. We note that the distribution function of (anti-)quarks belongs to the fundamental representation of the SU(3) gauge while that of gluons to the adjoint representation. Therefore, $i, j = 1, 2, 3$ and $a, b = 1, 2, ..., 8$.

Due to the average space-time homogeneity, the correlation tensor (1) depends only on the difference $(t_2 - t_1, \mathbf{x}_2 - \mathbf{x}_1)$. The space-time points $(t_1, \mathbf{x}_1)$ and $(t_2, \mathbf{x}_2)$ are correlated in the system of non-interacting particles if a particle travels from $(t_1, \mathbf{x}_1)$ to $(t_2, \mathbf{x}_2)$. For this reason the delta $\delta^{(3)}(\mathbf{x} - \mathbf{v}t)$ is present in the formula (1). The momentum integral of the distribution function simply represents the summation over particles. The fluctuation spectrum is found as a Fourier transform of the tensor (1) *i.e.*

$$M^{\mu\nu}_{ab}(\omega,\mathbf{k}) = \frac{1}{8}\, g^2\, \delta^{ab} \int \frac{d^3p}{(2\pi)^3}\, \frac{p^\mu p^\nu}{E_p^2}\, f(\mathbf{p})\, 2\pi\delta(\omega - \mathbf{k}\mathbf{v})\ . \qquad (2)$$

To compute the fluctuation spectrum, the parton momentum distribution has to be specified. Such calculations with two forms of the anisotropic momentum distribution are presented in [19]. Here I only qualitatively discuss Eqs. (1,2). I assume that the momentum distribution is elongated in, say, the z direction. Then, Eqs. (1,2) clearly show that the corelator M^{zz} is larger than M^{xx} or M^{yy}. It also clear that M^{zz} is the largest when the wave vector $\mathbf{k}$ is along the direction of the momentum deficit. Then, the delta function $\delta(\omega - \mathbf{k}\mathbf{v})$ does not much constrain the integral in Eq. (2). Since the momentum distribution is elongated in the z direction, the current fluctuations are the largest when the wave vector $\mathbf{k}$ is the $x-y$ plane. Thus, I conclude that some fluctuations in the anisotropic system are large, much larger than in the isotropic one and that anisotropic system has a natural tendency to split into the current filaments parallel to the direction of the momentum surplus. These currents are seeds of the filamentation instability.

2.2. Mechanism of filamentation

Let me now explain in terms of elementary physics why the fluctuating currents, which flow in the direction of the momentum surplus, can grow in time. To simplify the discussion, which follows [19], I consider an electromagnetic anisotropic system. The form of the fluctuating current is chosen to be

$$\mathbf{j}(x) = j\, \hat{\mathbf{e}}_z \cos(k_x x)\ , \qquad (3)$$

where $\hat{\mathbf{e}}_z$ is the unit vector in the z direction. As seen in Eq. (3), there are current filaments of the thickness $\pi/|k_x|$ with the current flowing in the opposite directions in the neighbouring filaments.

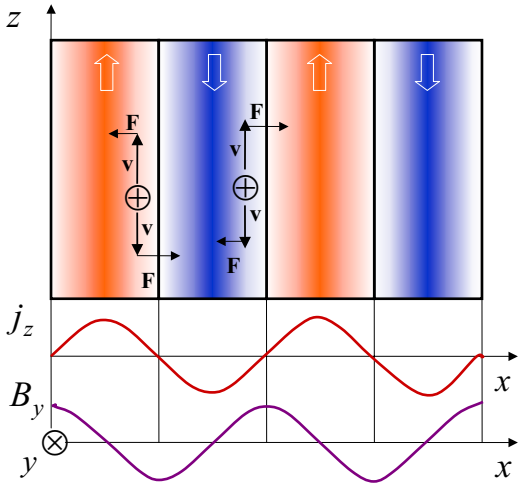

Figure 1. The mechanism of filamentation instability.

The magnetic field generated by the current (3) is given as

$$\mathbf{B}(x) = \frac{j}{k_x}\,\hat{\mathbf{e}}_y \sin(k_x x)\ ,$$

and the Lorentz force acting on the partons, which fly along the z direction, equals

$$\mathbf{F}(x) = q\,\mathbf{v}\times\mathbf{B}(x) = -q\,v_z\,\frac{j}{k_x}\,\hat{\mathbf{e}}_x \sin(k_x x)\ ,$$

where q is the electric charge. One observes, see Fig. 1, that the force distributes the partons in such a way that those, which positively contribute to the current in a given filament, are focused in the filament centre while those, which negatively contribute, are moved to the neighbouring one. Thus, the initial current is growing.

2.3. Dispersion equation

The Fourier transformed chromodynamic field $A^\mu(k)$ satisfies the equation of motion as

$$\Big[k^2 g^{\mu\nu} - k^\mu k^\nu - \Pi^{\mu\nu}(k)\Big] A_\nu(k) = 0\ , \tag{4}$$

where $\Pi^{\mu\nu}(k)$ is the polarization tensor or gluon self-energy which is discussed later on. A general plasmon dispersion equation is of the form

$$\det\Big[k^2 g^{\mu\nu} - k^\mu k^\nu - \Pi^{\mu\nu}(k)\Big] = 0\ . \tag{5}$$

Equivalently, the dispersion relations are given by the positions of poles of the effective gluon propagator. Due to the transversality of $\Pi^{\mu\nu}(k)$ ($k_\mu\Pi^{\mu\nu}(k) = k_\nu\Pi^{\mu\nu}(k) = 0$) not all components of $\Pi^{\mu\nu}(k)$ are independent from each other, and consequently the dispersion equation (5), which involves a determinant of 4×4 matrix, can be simplified to the determinant of 3×3 matrix. For this purpose I introduce the colour permittivity tensor $\epsilon^{lm}(k)$ where the indices $l, m, n = 1, 2, 3$ label three-vector and tensor components. Because of the relation

$$\epsilon^{lm}(k) E^l(k) E^m(k) = \Pi^{\mu\nu}(k) A_\mu(k) A_\nu(k)\ ,$$

where $\mathbf{E}$ is the chromoelectric vector, the permittivity can be expressed through the polarization tensor as

$$\epsilon^{lm}(k) = \delta^{lm} + \frac{1}{\omega^2}\Pi^{lm}(k)\ .$$

Then, the dispersion equation gets the form

$$\det\Big[\mathbf{k}^2\delta^{lm} - k^l k^m - \omega^2\epsilon^{lm}(k)\Big] = 0\,. \tag{6}$$

The relationship between Eq. (5) and Eq. (6) is most easily seen in the Coulomb gauge when $A^0 = 0$ and $\mathbf{k}\cdot\mathbf{A}(k) = 0$. Then, $\mathbf{E} = i\omega\mathbf{A}$ and Eq. (4) is immediately transformed into an equation of motion of $\mathbf{E}(k)$ which further provides the dispersion equation (6).

The dynamical information is contained in the polarization tensor $\Pi^{\mu\nu}(k)$ or, equivalently, in the permittivity tensor $\epsilon^{lm}(k)$ which can be derived either within the transport theory or diagrammatically [20]. The result is

$$\epsilon^{nm}(\omega,\mathbf{k}) = \delta^{nm} + \frac{g^2}{2\omega}\int\frac{d^3p}{(2\pi)^3}\frac{v^n}{\omega - \mathbf{kv} + i0^+}\frac{\partial f(\mathbf{p})}{\partial p^l}\left[\Big(1 - \frac{\mathbf{kv}}{\omega}\Big)\delta^{lm} + \frac{k^l v^m}{\omega}\right]. \tag{7}$$

Since $\Pi^{\mu\nu}(k)$ and $\epsilon^{lm}(k)$ are unit matrices in the colour space, the colour indices are suppressed here.

Substituting the permittivity (7) into Eq. (6), one fully specifies the dispersion equation (6) which provides a spectrum of quasi-particle bosonic excitations. A solution $\omega(\mathbf{k})$ of Eq. (6) is called *stable* when $\mathrm{Im}\omega \le 0$ and *unstable* when $\mathrm{Im}\omega > 0$. In the first case the amplitude is constant or it exponentially decreases in time while in the second one there is an exponential growth of the amplitude. In practice it appears difficult to find solutions of Eq. (6) because of rather complicated structure of the tensor (7). However, the problem simplifies as we are interested in specific modes which are expected to be unstable. Namely, we look for solutions corresponding to the fluctuating current in the direction of the momentum surplus and the wave vector perpendicular to it.

As previously, the momentum distribution is assumed to be elongated in the z direction, and consequently the fluctuating current also flows in this direction. The magnetic field has a non-vanishing component along the y direction and the electric filed in the z direction. Finally, the wave vector is parallel to the axis x, see Fig. 1. We also assume that the momentum distribution obeys the mirror symmetry $f(-\mathbf{p}) = f(\mathbf{p})$, and then the permittivity tensor has only non-vanishing diagonal components. Taking into account all these conditions, one simplifies the dispersion equation (6) to the form

$$H(\omega) \equiv k_x^2 - \omega^2\epsilon^{zz}(\omega,k_x) = 0\ , \tag{8}$$

where only one diagonal component of the dielectric tensor enters.

It appears that an existence of unstable solutions of Eq. (8) can be proved without solving it. The so-called Penrose criterion [22], which follows from analytic properties of the permittivity as a function of ω, states that *the dispersion equation $H(\omega) = 0$ has unstable solutions if $H(\omega = 0) < 0$*. The Penrose criterion was applied to the equation (8) in [11] but a much more general discussion of the instability condition is presented in [16]. Not entering into details, there exist unstable modes if the momentum distribution averaged (with a proper weight) over momentum length is anisotropic.

To solve the dispersion equation (8), the parton momentum distribution has to be specified. Several analytic (usually approximate) solution of the dispersion equation with various momentum distributions can be found in [11, 15, 16]. An example of the numerical solution,

which gives the unstable mode frequency in the full range of wave vectors is shown Fig. 2 taken from [14]. The momentum distribution is of the form

$$f(\mathbf{p}) \sim \frac{1}{(p_T^2+\sigma_\perp^2)^3}\, \mathrm{e}^{-\frac{p_z^2}{2\sigma_\parallel^2}} ,$$

where $p_\perp \equiv \sqrt{p_x^2+p_y^2}$. The mode is pure imaginary and $\gamma_k \equiv \mathrm{Im}\omega(k_\perp)$. The value of the coupling is $\alpha_s \equiv g^2/4\pi = 0.3$, $\sigma_\perp = 0.3$ GeV and the effective parton density is chosen to be 6 fm^{-3}. As seen, there is a finite interval of wave vectors for which the unstable modes exist.

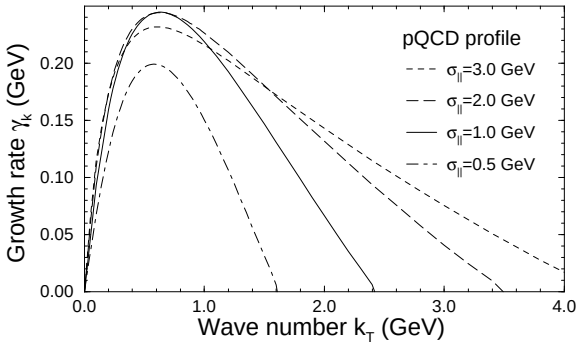

Figure 2. The growth rate of the unstable mode as a function of the wave vector k $= (k_\perp, 0, 0)$ for $\sigma_\perp = 0.3$ GeV and 4 values of the parameter $\sigma_\parallel$ which controls system's anisotropy. The figure is taken from [14].

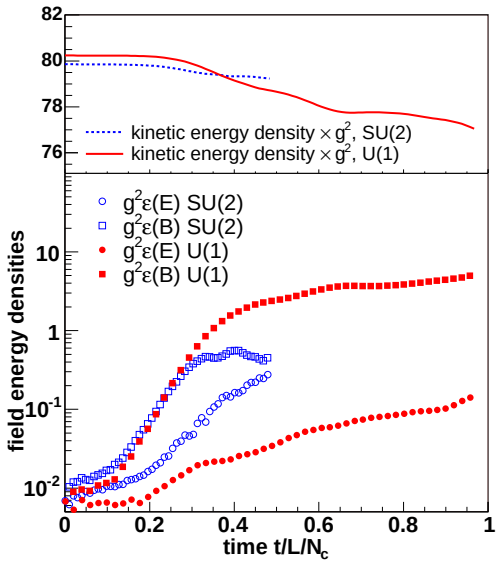

Figure 3. Time evolution of the kinetic energy of particles (upper panel) and the energy stored in electric and magnetic fields (lower panel) in GeV/fm^3 for the U(1) and SU(2) gauge groups. The figure is taken from [17].

2.4. Growth of instabilities and abelianization

A time evolution of a classical many-parton system interacting via classical chromodynamic field has been studied in [17]. Numerical simulations have been performed effectively in $1+1$ dimensions as the chromodynamic potentials depend on t and x. The initial field amplitudes are assumed to obey Gaussian white noise and the initial parton momentum distribution is

$$f(\mathbf{p}) \sim \delta(p_z)\, \mathrm{e}^{-\frac{\sqrt{p_x^2+p_y^2}}{p_{\mathrm{hard}}}} , \qquad (9)$$

with $p_{\mathrm{hard}} = 10$ GeV.

Fig. 3, which is taken from [17], shows results of the simulation corresponding to a lattice of physical size $L = 40$ fm. As seen, the amount of energy of the fields, which is initially much smaller than the kinetic energy of all particles, grows exponentially and the magnetic contribution dominates. The simulation [17] indirectly confirms existence of the unstable magnetic modes in the system.

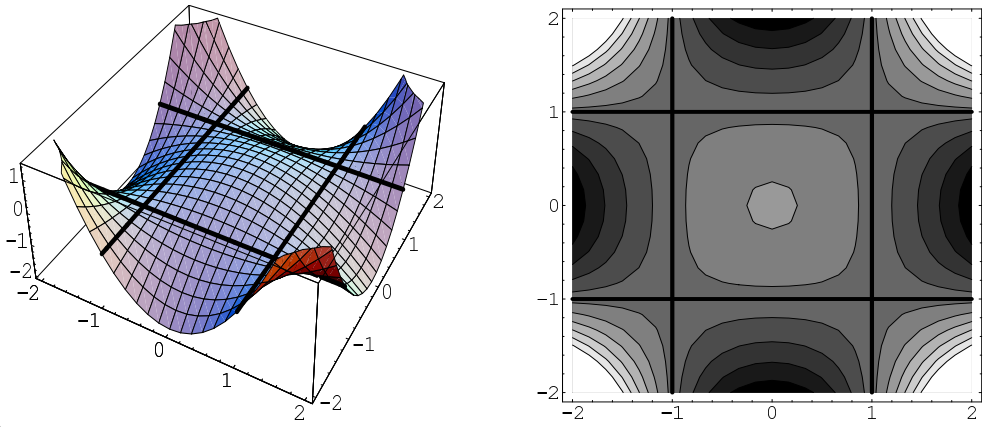

Figure 4. The effective potential of the unstable magnetic mode as a function of two colour components of $\mathbf{A}^a$ belonging to the SU(2) gauge group. The figure is taken from [21].

Unstable modes cannot grow to infinity and the question arises what is a mechanism responsible for stopping the instability growth. One suspects that non-Abelian non-linearities can play an important role here. An elegant qualitative argument [21] suggests that the non-linearities do not stabilize the unstable modes because the system spontaneously chooses an Abelian configuration in the course of the instability development. Let me explain the idea.

In the Coulomb gauge the effective potential of the unstable configuration has the form

$$V_{\rm eff}[\mathbf{A}^a] = -\mu^2 \mathbf{A}^a \cdot \mathbf{A}^a + \frac{1}{4} g^2 f^{abc} f^{ade} (\mathbf{A}^b \mathbf{A}^d)(\mathbf{A}^c \mathbf{A}^e) \; ,$$

which is shown in Fig. 4 taken from [21]. The first term (with $\mu^2 > 0$) is responsible for a very existence of the instability. The second term, which comes from the Yang-Mills lagrangian, is of pure non-Abelian nature. The term appears to be positive and thus it counteracts the instability growth. However, the non-Abelian term vanishes when the potential $\mathbf{A}^a$ is effectively Abelian, and consequently, such a configuration corresponds to the steepest decrease of the effective potential. Thus, the system spontaneously abelianizes in the course of instability growth.

The effect of abelianization has been indeed found in numerical simulations performed in the $1+1$ dimensions [12, 17, 21]. As an example, I show in Fig. 5 the result of fully classical simulation [17]. One observes in Fig. 5 taken from [17], where

$$\phi_{\rm rms} \equiv \sqrt{\int_0^L \frac{dx}{L} (A_y^a A_y^a + A_z^a A_z^a)} \; , \qquad \bar{C} \equiv \int_0^L \frac{dx}{L} \frac{\sqrt{{\rm Tr}[(i[A_y, A_z])^2]}}{{\rm Tr}[A_y^2 + A_z^2]} \; ,$$

that the field commutator measured by $\bar{C}$ decreases in time, in spite of the field growth quantified by $\phi_{\rm rms}$.

Very recent simulations performed in the $1+3$ dimensions [23, 24], which utilise a complete Hard Loop action for anisotropic systems [25], show that the growth of unstable modes, which is initially exponential, becomes only linear at the later times. And the abelianization works only in the exponential period of instability development. However, it might well be that the abelianization becomes more efficient when the dynamical effects beyond the Hard Loop approximation are taken into account [26].

2.5. Isotropization

When instabilites grow the systems becomes more isotropic because the Lorentz force acts on particle's momenta and the growing fields generate an extra momentum.

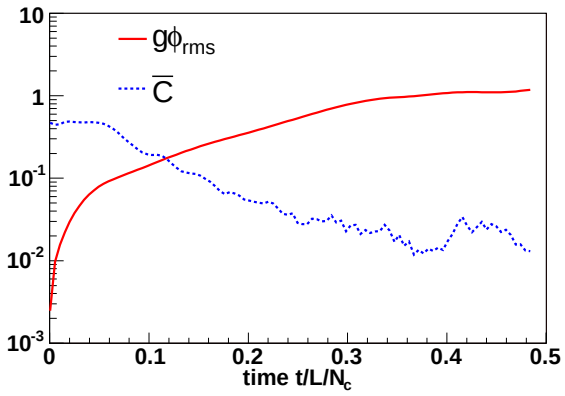

Figure 5. Temporal evolution of $\bar{C}$ and $\phi_{\rm rms}$ measured in GeV. The figure is taken from [17].

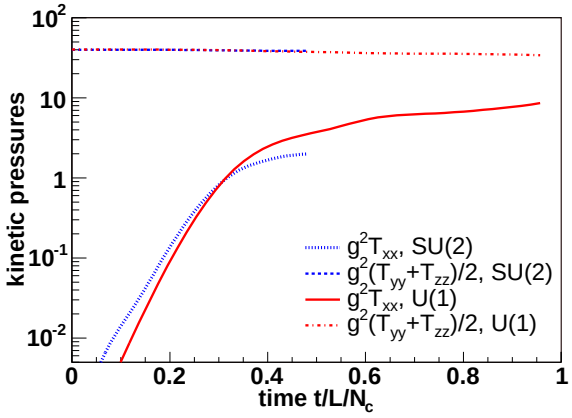

Figure 6. Temporal evolution of T^{xx} and $(T^{yy}+T^{zz})/2$. The figure is taken from [17].

To explain the mechanism I assume, as previously, that initially there is a momentum surplus in the z direction. The fluctuating current tends to flow in the z direction with the wave vector pointing in the x direction. Since the magnetic field has a y component, the Lorentz force, which acts on partons flying along the z axis, pushes the partons in the x direction where there is a momentum deficit.

The effect of isotropization due to the action of the Lorentz force is nicely seen in the classical simulation [17]. In Fig. 6, which is taken from [17], there are shown diagonal components of the energy-momentum tensor

$$T^{\mu\nu} = \int \frac{d^3p}{(2\pi)^3}\frac{p^\mu p^\nu}{E_p} f(\mathbf{p}) \; .$$

The initial momentum distribution is given by Eq. (9), and consequently $T^{xx} = 0$ at $t = 0$. As seen in Fig. 6, T^{xx} exponentially grows.

The system isotropizes not only due to the effect of the Lorentz force but also due to the momentum carried by the growing field. As explained in detail in [11], the momentum of the field is oriented along the wave vector which points in the direction of the momentum deficit. This effect has not been numerically studied yet but it is clear that the effect is comparable to that of Lorentz force only for suffuciently large field amplitudes.

3. Azimuthal fluctuations

In the first part of my talk I have argued that the quark-gluon plasma becomes isotropic fast due to the magnetic instabilities. And it has been recently observed [13] that the system with isotropic momentum distribution manifests a hydrodynamic collective behaviour. The question arises whether such an approximate hydrodynamics can be distinguished from the real hydrodynamics describing a system which is in a local thermodynamic equilibrium. In the second part of my talk I propose to address the question by studying the azimuthal fluctuations.

In relativistic heavy-ion collisions both at CERN SPS and BNL RHIC, one observes a sizable elliptic flow which is quantified by the second angular harmonics v_2 of the azimuthal distribution of final state hadrons [2, 3, 4, 5]. The phenomenon, which is sensitive to the collision early stage [8] when the interaction zone is of the almond shape, is naturally explained within a hydrodynamics as a result of large density gradients [27, 28, 29, 30]. Hydrodynamic description requires that the system under study is in a local thermodynamical equilibrium. However, an approximate hydrodynamic behaviour occurs, as argued in [13], when the momentum distribution of liquid components is merely isotropic in the local rest frame. The point is

that the structure of the ideal fluid energy-momentum tensor *i.e.* $T^{\mu\nu} = (\varepsilon + p)\, u^\mu u^\nu - p\, g^{\mu\nu}$, where ε, p and u^μ is the energy density, pressure and hydrodynamic velocity, respectively, holds for an arbitrary, though isotropic momentum distribution. ε and p are then not the energy density and pressure but the moments of the distribution function which are equal the energy density and pressure in the equilibrium limit. Since the tensor $T^{\mu\nu}$ obeys the continuity equation $\partial_\mu T^{\mu\nu} = 0$, one gets an analogue of the Euler equation. However, due to the lack of thermodynamic equilibrium there is no entropy conservation and the equation of state is missing.

Usually, non-equilibrium fluctuations are significantly smaller than the equilibrium fluctuations of the same quantity. A specific example of such an situation has been discussed in Sec. 2.1. Therefore, I expect that the fluctuations of v_2 produced in the course of real hydrodynamic evolution are significantly smaller than those generated in the non-equilibrium quark-gluon plasma which is merely isotropic. It should be stressed here that the elliptic flow is generated in the collision early stage. Thus, I propose to carefully measure the fluctuations of v_2 as discussed in [31]. Since such a measurement is rather difficult, I also consider an integral measurement of azimuthal fluctuations proposed in [32] which can also help to distinguish the equilibrium from non-equilibrium fluctuations.

3.1. Elliptic flow fluctuations

In my discussion of v_2 fluctuations I follow [31] where the standard method [33, 34] to measure the elliptic flow was used. The method focuses on the angular distributions relative to direction of the impact parameter. The experimental procedure splits in two steps which should be as independent as possible. In the first step, one determines the impact parameter direction ψ_R, while in the second step, one constructs the distribution of azimuthal angle relative to ψ_R and one computes the Fourier coefficients.

The one-particle distribution in a single event can be written as

$$P_{\rm ev}(\phi) = \frac{1}{2\pi}\,\Big[1 + 2\sum_{n=1}^{\infty} v_n \cos(n(\phi - \psi_R))\Big]\Theta(\phi)\,\Theta(2\pi - \phi)\ . \tag{10}$$

Since the reaction plane is never reconstructed precisely and the real reaction plane angle ψ_R deviates from the estimated angle ψ_E, the $n-$th Fourier amplitude v_n is determined as

$$v_n = \frac{1}{R_n}\,\overline{\cos(n(\phi - \psi_E))}\ ,$$

where $R_n \equiv \cos(n(\psi_R - \psi_E))$ is the reaction plane resolution factor and $\overline{\cdots}$ denotes averaging over particles from a single event.

Let me now consider an ensemble of events with every event representing a single nucleus-nucleus collision at fixed value (not direction) of the impact parameter. The angle ψ_R (and ψ_E) obviously varies form event to event. The question is how to detect the event-by-event fluctuations of the Fourier amplitudes v_n. According to [34], the amplitude averaged over events is defined as

$$\langle v_n \rangle \stackrel{\rm def}{=} \frac{\Big\langle \overline{\cos(n(\phi - \psi_E))} \Big\rangle}{\langle R_n \rangle}\ ,$$

where $\langle \cdots \rangle$ denotes averaging over events. We define the second moment as

$$\langle v_n^2 \rangle \stackrel{\rm def}{=} \frac{1}{\langle R_n \rangle^2} \Big\langle \overline{\cos(n(\phi - \psi_E))}^2 \Big\rangle\ ,$$

and the fluctuations are

$$\mathsf{Var}(v_n) \equiv \langle v_n^2 \rangle - \langle v_n \rangle^2 = \frac{1}{\langle R_n \rangle^2} \Big(\Big\langle \overline{\cos(n(\phi - \psi_E))}^2 \Big\rangle - \Big\langle \overline{\cos(n(\phi - \psi_E))} \Big\rangle^2 \Big)\ .$$

There are several sources of trivial v_2 fluctuations which are not related to the system's dynamics of interest. I start with the fluctuations caused by a varying number of particles used to determine ψ_E and v_2. I assume here that the Fourier amplitudes v_n do *not* change from event to event and that the only correlations in the system are those due to the flow. Then, the azimuthal distribution of N particles is a product of N single particle distributions

$$P^N_{\rm ev}(\phi_1,\phi_2,\cdots,\phi_N) = \mathcal{P}_N P_{\rm ev}(\phi_1)\, P_{\rm ev}(\phi_2)\, \cdots\, P_{\rm ev}(\phi_N)\,, \tag{11}$$

where $\mathcal{P}_N$ is the multiplicity distribution while all distributions $P_{\rm ev}(\phi_i)$ are given by Eq. (10). The single particle distributions $P_{\rm ev}(\phi_i)$ are correlated to each other because of the common angle ψ_R.

Using the distribution (11), one finds (neglecting v_4) the variance of v_2 as

$$\mathsf{Var}(v_2) = \frac{1}{2\langle R_2\rangle^2\langle N\rangle} + \langle v_2\rangle^2\, \frac{\langle R_2^2\rangle - \langle R_2\rangle^2}{\langle R_2\rangle^2}\,, \tag{12}$$

which holds for $\langle N\rangle \gg 1$ and small multiplicity fluctuations. The second term in r.h.s of Eq. (12) appears to be much smaller than the first one as $\langle R_2^2\rangle - \langle R_2\rangle^2 \sim \langle M\rangle^{-2}$, where M is the number of particles used to determine the reaction plane and M is assumed to be of the same order as N. Thus, the statistical noise contribution to $\delta v_2 \equiv \sqrt{\mathsf{Var}(v_2)}$ is finally estimated as

$$\delta v_2 = \frac{1}{\langle R_2\rangle\sqrt{2\langle N\rangle}}\,. \tag{13}$$

As well known, $\langle v_2\rangle$ strongly depends on the collision impact parameter b. Using the parameterisation of this dependence given in [3], one computes δv_2 as $(d\langle v_2\rangle/db)\delta b$. The impact parameter is measurable through the multiplicity N_p of participating nucleons. N_p is directly related to b. For $b \approx 10$ fm, when the flow in Au-Au collisions is maximal, the v_2 fluctuations due to the impact parameter variation vanish because $d\langle v_2\rangle/db = 0$. For $b = 5$ fm, where $\langle v_2\rangle \approx 0.03$, one finds $\delta v_2 \approx 8\cdot 10^{-4}\,\delta N_p$. When $\delta N_p = 30$ and $\langle N\rangle = 500$, the magnitude of the v_2 fluctuations caused by the impact parameter variation is approximately equal to that of the statistical noise.

The next source of trivial v_2 fluctuations is a variation of thermodynamic parameters. The contribution caused by the particle number fluctuations can be estimated as

$$\delta v_2 = \frac{d\langle v_2\rangle}{d\langle N\rangle}\,\delta N = \langle v_2\rangle\,\frac{\delta N}{\langle N\rangle} P\,,$$

where the effective power P is

$$P \equiv \frac{d\ln\langle v_2\rangle}{d\ln\langle N\rangle} = \frac{\langle N\rangle}{\langle v_2\rangle}\,\frac{d\langle v_2\rangle}{d\langle N\rangle}\,.$$

Assuming the poissonian character of multiplicity fluctuations, one obtains

$$\delta v_2 = \frac{\langle v_2\rangle}{\sqrt{\langle N\rangle}}\,P\,. \tag{14}$$

The value of the index P can be estimated within the hydrodynamic model [29] as $P \approx 0.4$. Comparing Eqs. (13) and (14), one finds that the ratio of the thermodynamic fluctuations to the statistical noise, is 0.04 for $\langle v_2\rangle = 0.07$ and $P = 0.4$. Thus, the thermodynamic fluctuations are much smaller than the statistical noise.

Concluding this section, I propose to perform a systematic measurement of event-by-event v_2 fluctuations for the centrality corresponding to the maximal elliptic flow. Then, the fluctuations caused by the impact parameter variation vanish or at least they are very small. If the flow is built up in the course of hydrodynamic evolution of the equilibrium system, v_2 should be dominated by the statistical noise related to the finite particle number. The noise can be identified due to the characteristic $1/\langle N\rangle$ dependence.

3.2. Φ measure of azimuthal fluctuations

Since a measurement of v_2 fluctuations discussed in the previous section is rather difficult, I suggest to consider a much simpler integral measurement of azimuthal fluctuations [32], using the so-called Φ measure introduced in [35].

The correlation (or fluctuation) measure Φ is defined as follows. One defines the variable $z \stackrel{\rm def}{=} x - \overline{x}$, where x is a single particle characteristics such as the particle transverse momentum or the azimuthal angle. In this section the overline does not denote averaging over particles from a single event but averaging over a single particle inclusive distribution. x is identified here with the particle azimuthal angle. The event variable Z, which is a multiparticle analog of z, is defined as $Z \stackrel{\rm def}{=} \sum_{i=1}^{N}(x_i - \overline{x})$, where the summation runs over particles from a given event. By construction, $\langle Z \rangle = 0$. The measure Φ is finally defined as

$$\Phi \stackrel{\rm def}{=} \sqrt{\frac{\langle Z^2 \rangle}{\langle N \rangle}} - \sqrt{\overline{z^2}} \, .$$

Φ obviously vanishes in the absence of any inter-particle correlations. Other properties of Φ are discussed in [36].

The Φ measure is sensitive to the azimthal fluctuations caused by the transverse collective flow. Let me compute it, assuming that the only correlations present in the system are due to the collective flow. The inclusive ϕ distrubtion, which is flat in the range $[0, 2\pi]$, provides $\overline{\phi} = \pi$ and $\overline{\phi^2} = \frac{4}{3}\pi^2$, and consequently, $\overline{z^2} = \frac{1}{3}\pi^2$. Since $Z = \sum_{i=1}^{N}(\phi_i - \overline{\phi})$, one computes $\langle Z^2 \rangle$, using the event distribution (10), as

$$\langle Z^2 \rangle = \int_0^{2\pi} \frac{d\psi_R}{2\pi} \sum_N \mathcal{P}_N \int_0^{2\pi} d\phi_1 \ldots \int_0^{2\pi} d\phi_N \; P_{\rm ev}(\phi_1) \; \ldots \; P_{\rm ev}(\phi_N) \; (\phi_1 + \ldots + \phi_N - N\overline{\phi})^2 \, . \quad (15)$$

The averaging over the amplitudes v_n, which is not shown here, is implied. At first glance, the multi-particle distribution from Eq. (15) might look as a simple product of one-particle distributions. One should note however that every $P_{\rm ev}(\phi)$ depends on the reaction plane angle ψ_R, and the integration over ψ_R leads to the *correlated* multi-particle distribution.

After elementary calculation, one finds for small v_n, poissonian multiplicity distribution and $\langle N \rangle \gg 1$, an approximate expression of interest

$$\Phi \cong \frac{3}{\pi^2} \, \langle N \rangle \, \langle \sum_{n=1}^{\infty} (\frac{v_n}{n})^2 \rangle \, . \quad (16)$$

If all amplitudes v_n except v_2 vanish, as it approximately happens in the central rapidity domain, and v_2 equals a unique value 0.07, Eq. (16) for $\langle N \rangle = 500$ gives $\Phi = 0.2$.

As already mentioned, the transverse flow is far not the only source of the azimuthal fluctuations. In particular, the effect of quantum statistics contribute here. To estimate the effect one computes Φ in the equilibrium ideal quantum gas. The result reads [32]

$$\Phi = \frac{\pi}{\sqrt{3}} \Big(\sqrt{\frac{\widetilde{\rho}}{\rho}} - 1 \Big) \, , \quad (17)$$

where

$$\rho \equiv \int \frac{d^3p}{(2\pi)^3} \, \frac{1}{\lambda^{-1} e^{\beta E_p} \pm 1} \, , \qquad \widetilde{\rho} \equiv \int \frac{d^3p}{(2\pi)^3} \, \frac{\lambda^{-1} e^{\beta E_p}}{(\lambda^{-1} e^{\beta E_p} \pm 1)^2} \, ,$$

λ denotes the fugacity, the upper sign is for fermions and the lower one for bosons. As seen, Φ is independent of the system's volume and of the number of particle's internal degrees of freedom.

For massless bosons with vanishing chemical potential, Eq. (17) gives $\Phi \approx 0.3$ for any T. More realistic calculations [32] provide $\Phi \approx 0.06$ for chemically equilibrated pions at $T = 150$ MeV.

I conclude this section by saying that a measured value of Φ, which would significantly exceed predictions of Eq. (16) with non-fluctuating amplitudes v_n, would be an obvious signal of sizable dynamical fluctuations.

4. Final remarks

The magnetic instabilities provide a plausible mechanism responsible for a surprisingly short equilibration time observed in relativistic heavy-ion collisions. Fast isotropization is a distinctive feature of the mechanism. It is certainly desirable to look for experimentally detectable signals of the instabilities driven thermalization. In my talk I have proposed to study azimuthal fluctuations, in particular the event-by-event fluctuations of the elliptic flow which is generated at the collision early stage. I have not been able to present a quantitative prediction but observation of sizeable dynamical fluctuations would be a strong argument that behind a smooth hydrodynamic evolution there is a violent phenomenon of plasma instabilities.

[1] Heinz U 2005 Equation of state and collective dynamics *Preprint* nucl-th/0504011
[2] Alt C et al 2003 *Phys. Rev.* C **68** 034903
[3] Adler C et al 2002 *Phys. Rev.* C **66** 034904
[4] Adler S S et al 2003 *Phys. Rev. Lett.* **91** 182301
[5] Back B B et al 2005 *Phys. Rev. Lett.* **94** 122303
[6] Heinz U W 2005 *AIP Conf. Proc.* **739** 163
[7] Shuryak E 2004 *J. Phys.* G **30** S1221
[8] Sorge H 1999 *Phys. Rev. Lett.* **82** 2048
[9] Baier A, Mueller A H, Schiff D and Son D T 2002 *Phys. Lett.* B **539** 46
[10] Arnold P, Son D T and Yaffe L G 1999 *Phys. Rev.* D **59** 105020
[11] Mrówczyński St 1994 *Phys. Rev.* C **49** 2191
[12] Rebhan A, Romatschke P and Strickland M, *Phys. Rev. Lett.* **94** 102303
[13] Arnold P, Lenaghan J, Moore G D and Yaffe L G 2005 *Phys. Rev. Lett.* **94** 072302
[14] Randrup J and Mrówczyński St 2003 *Phys. Rev.* C **68** 034909
[15] Romatschke P and Strickland M 2003 *Phys. Rev.* D **68** 036004
[16] Arnold P, Lenaghan J and Moore G D 2003 *JHEP* **0308** 002
[17] Dumitru A and Nara Y 2005 QCD plasma instabilities and isotropization *Preprint* hep-ph/0503121
[18] Weibel E S 1959 *Phys. Rev. Lett.* **2** 83
[19] Mrówczyński St 1997 *Phys. Lett.* B **393** 26
[20] Mrówczyński St and Thoma M H 2000 *Phys. Rev.* D **62** 036011
[21] Arnold P and Lenaghan J 2004 *Phys. Rev.* D **70** 114007
[22] Krall N A and Trivelpiece A W 1973 *Principles of Plasma Physics* (New York: McGraw-Hill)
[23] Arnold P, Moore G D and Yaffe L G 2005 The fate of non-abelian plasma instabilities in 3+1 dimensions *Preprint* hep-ph/0505212
[24] Rebhan A, Romatschke P and Strickland M 2005 Dynamics of quark-gluon plasma instabilities in discretized hard-loop approximation *Preprint* hep-ph/0505261
[25] Mrówczyński St, Rebhan A and Strickland M 2004 *Phys. Rev.* D **70** 025004
[26] Manuel C and Mrówcźnski St 2005 Strongly and weakly unstable anisotropic quark-gluon plasma *Preprint* hep-ph/0504156
[27] Ollitrault J Y 1992 *Phys. Rev.* D **46** 229
[28] Kolb P F, Sollfrank J and Heinz U W 2000 *Phys. Rev.* C **62** 054909
[29] Teaney D, Lauret J and Shuryak E V 2001 A hydrodynamic description of heavy ion collisions at the SPS and RHIC *Preprint* nucl-th/0110037
[30] Hirano T 2002 *Phys. Rev.* C **65** 011901
[31] Mrówczyński St and Shuryak E V 2003 *Acta Phys. Polon.* B **34** 4241
[32] Mrówczyński St 2000 *Acta Phys. Polon.* B **31** 2065
[33] Voloshin S A and Zhang Y 1996 *Z. Phys. C* **70** 665
[34] Poskanzer A M and Voloshin S A 1998 *Phys. Rev.* C **58** 1671
[35] Gaździcki M and Mrówczyński St 1992 *Z. Phys.* C **54** 127
[36] Mrówcźnski St 1999 *Phys. Lett.* B **465** 8